

Vibrational and NMR Investigation on Pharmaceutical Activity of 2,5-Dimethoxy-4-Ethylamphetamine by Theoretical and Experimental Support

A Madanagopal¹, S Periandy², P Gayathri¹, S Ramalingam^{3*} and S Xavier⁴

¹Department of Physics, Periyar Maniammai University, Thanjavur, Tamilnadu, India

²Department of Physics, Kanchi Mamunivar Centre for PG studies, Puducherry, India

³PG and Research Department of Physics, A.V.C. College, Mayiladuthurai, Tamilnadu, India

⁴Department of Physics, St. Joseph College of Arts and Science, Cuddalore, Tamil Nadu, India

*Corresponding author: S Ramalingam, PG and Research Department of Physics, A.V.C. College, Mayiladuthurai, Tamilnadu, India, Tel: 04364 222264; Fax: 04364 222264; E-mail: ramalingam.physics@gmail.com

Received Date: January 31, 2017, Accepted Date: February 28, 2017, Published Date: March 07, 2017

Copyright: © 2017 Madanagopal A, et al. This is an open-access article distributed under the terms of the Creative Commons Attribution License, which permits unrestricted use, distribution, and reproduction in any medium, provided the original author and source are credited.

Abstract

The Detailed physical, chemical, thermal and circular vibrational investigations have been made on FT-IR, FT-Raman, NMR and UV-Visible spectra of 2,5-Dimethoxy-4-ethylamphetamine. The modification of the basic property (deficit hyperactivity disorder) of the base compound (Amphetamine) is favoured by the insertion of two methoxy and ethyl-methyl groups have been discussed in detail. The transitional pattern among NBO emphasized the inducement of the psychedelic activity in the compound. The strong interpretation made on the physical and chemical properties by intense observation using excitations between the electronic energy levels within the molecule have been carried out. The arrangement of the dipole moment of the bonds and the change of resultant magnetic moment were observed from the average Polarizability first order diagonal hyperpolarizability. The receptor and inhibition property of the molecule were interpreted by the identification of reactive sites from molecular electrostatic potential contour map. The chemical reaction continuity is keenly observed from thermodynamical analysis.

Keywords: 2,5-Dimethoxy-4-Ethylamphetamine; Amphetamine; Transitional Pattern; Hyperactivity Disorder; Amphetamine; Chemical Reaction Continuity

Introduction

The 2,5-Dimethoxy-4-ethylamphetamine is commonly known as substituted amphetamines and is a psychedelic(also known as psychotogenic) drug [1,2]. It has an active stereocenter which is more active enantiomer and it is a potent and long-acting psychedelic [3,4].

The compound is composed systematically and heavily by methoxy, methyl, ethyl and amino substitutions. Two methoxy groups are loaded symmetrically at ortho and meta positions of left and right moiety respectively of the benzene ring. Similarly, the chain of ethyl and methyl groups substituted at ortho in right moiety whereas the chain of ethyl and methyl groups along with amino ligand present at meta position of left moiety.

The benzene ring with chain of CH, CH₂, CH₃, and NH₂ groups forms alpha-methylphenethylamine called as Amphetamine. It is a potent drug which stimulant central nervous system (CNS) and is used for the treatment of attention deficit hyperactivity disorder, narcolepsy and obesity [5,6]. The compound; Amphetamine drug existed in two enantiomer forms, such as levoamphetamine and dextroamphetamine.

Historically, it has been used to treat nasal congestion and depression. Amphetamine is also used as an athletic performance enhancer and cognitive enhancer, and recreationally as an aphrodisiac and euphoriant. Hence, when the Amphetamine is substituted by symmetrical insertion of two methoxy and asymmetrical addition of

ethyl-methyl groups, the composite compound is changed as psychotogenic drug.

In spite of its important pharmaceutical applications thereof; 2,5-Dimethoxy-4-ethylamphetamine has not been subjected to systematic investigation on the structure activity related to its pharmaceutical potential. Therefore, the present investigation is made for the strong interpretation on the structure activity associated with active drug property of the compound using FT-IR, FT-Raman, NMR and UV-Visible spectroscopical data and computational results.

Experimental Profile

Physical state

The compound has been taken in solid form which is pure and spectroscopic grade.

Recording profile

The FT-IR and FT-Raman spectra of the compound were recorded using a Bruker IFS 66V spectrometer and the instrument adopted with an FRA 106 Raman module equipped with aNd:YAG laser source operating at 1.064 μm line widths with 200 mW power [7].

The high resolution ¹HNMR and ¹³CNMR spectra were recorded using 300 MHz and 75 MHz FT-NMR spectrometer [8].

The UV-Vis spectrum was recorded in the range of 200 nm to 800 nm, with the scanning interval of 0.2 nm, using the UV-1700 series instrument [9].

Computational Profile

In order to design the structure precisely, calculate geometrical parameters, display the Mulliken charge levels, study the vibrational spectral properties, observe the molecular orbital interactions, examine the frontier molecular transitions on the electronic structure, the entire quantum chemical computations were performed using the Gaussian 09 D. 01. version software program in core i7 computer [10].

The computational calculations were performed over entire geometrical parameters, vibrational frequencies, simulation of molecular structure and spectra using B3LYP and B3PW91 methods adopted with 6-31++G(d, p) and 6-311++G(d,p) basis sets (Table 1). The energy absorbance by the present compound related with

electronic spectra, the NBO and HOMO-LUMO energies were calculated using time-dependent SCF method with best fit basis set. In the same way, the ¹H and ¹³C NMR chemical shifts with respect to TMS were calculated by GIAO method using I-PCM model in combination with B3LYP/6-311++G(2d,p). The Mulliken charge assignment on different parts of the compound was calculated and was purposely elucidated for the determination of key factor for pharmaceutical activity of the compound. The dipole moment, linear polarizability and the first order hyper polarizability in different coordinates of the compound were computed using B3LYP method with the 6-311++G(d,p) basis set. The ECD and VCD spectra were simulated from available frequencies and the optical chirality was studied and the mechanism for masking the toxicity was interpreted.

Geometrical Parameters	Methods			
	HF/6-311++G(d,p)	B3LYP/6-311++G(d,p)	CAM-B3LYP/6-311++G(d,p)	B3PW91/6-311++G(d,p)
Bond length(Å)				
C1-C2	1.391	1.404	1.402	1.4
C1-C6	1.386	1.397	1.396	1.394
C1-O12	1.381	1.403	1.374	1.367
C2-C3	1.39	1.401	1.397	1.395
C2-C13	1.511	1.511	1.51	1.505
C3-C4	1.386	1.397	1.396	1.394
C3-H7	1.071	1.08	1.082	1.083
C4-C5	1.39	1.404	1.402	1.4
C4-O10	1.381	1.403	1.375	1.368
C5C-6	1.389	1.4	1.396	1.394
C5-C9	1.511	1.513	1.511	1.506
C6-H8	1.071	1.08	1.082	1.084
H7-H26	3.229	3.24	1.093	1.094
C9-H14	1.082	1.091	1.094	1.095
C9-H15	1.085	1.093	1.539	1.532
C9-C34	1.536	1.543	1.418	1.41
O10-C11	1.426	1.449	1.096	1.097
C11-H16	1.082	1.092	1.096	1.096
C11-H17	1.082	1.092	1.089	1.09
C11-H18	1.076	1.085	1.418	1.41
O12-C30	1.426	1.449	1.092	1.093
C13-H19	1.08	1.089	1.097	1.097
C13-H20	1.087	1.096	1.544	1.538
C13-C21	1.541	1.549	1.093	1.095
C21-H22	1.081	1.091	1.535	1.53

C21-C23	1.535	1.54	1.473	1.466
C21-N27	1.461	1.475	1.094	1.094
C23-H24	1.085	1.092	1.096	1.097
C23-H25	1.087	1.095	1.093	1.094
C23-H26	1.083	1.091	1.015	1.014
N27H28	0.995	1.012	1.017	1.016
N27H-29	0.997	1.014	1.096	1.097
C30-H31	1.082	1.092	1.095	1.096
C30-H32	1.082	1.092	1.089	1.09
C30-H33	1.076	1.085	1.092	1.092
C34-H35	1.082	1.089	1.094	1.094
C34-H36	1.085	1.092	1.093	1.094
C34-H37	1.084	1.092	1.093	1.089
Bond angle(°)				
C2-C1-C6	120.784	120.931	120.213	120.137
C2-C1-O12	116.171	115.552	116.033	116.079
C6-C1-O12	123.044	123.515	123.752	123.781
C1-C2-C3	117.628	117.577	117.892	117.935
C1-C2-C13	121.133	120.971	120.945	120.851
C3-C2-C13	121.23	121.448	121.159	121.211
C2-C3-C4	121.599	121.493	121.888	121.917
C2-C3-H7	118.212	118.041	117.895	117.846
C4-C3-H7	120.187	120.464	120.215	120.234
C3-C4-C5	120.706	120.874	120.181	120.107
C3-C4-O10	123.173	123.619	123.791	123.808
C5-C4-O10	116.119	115.505	116.026	116.083
C4-C5-C6	117.77	117.697	117.981	118.026
C4-C5-C9	121.15	120.971	121.092	120.994
C6-C5-C9	121.076	121.325	120.92	120.972
C1-C6-C5	121.509	121.423	121.841	121.872
C1-C6-H8	120.213	120.461	120.226	120.232
C5-C6-H8	118.277	118.114	117.931	117.894
C3-H7-H26	73.274	72.766	109.291	109.233
C5-C9-H14	109.292	109.165	108.782	108.799
C5-C9-H15	108.884	108.96	113.286	113.092
C5-C9-C34	112.966	113.257	106.967	106.921

H14-C9-H15	107.182	107.132	108.959	109.087
H14-C9-C34	109.046	108.777	109.359	109.519
H15-C9-C34	109.303	109.365	109.78	118.315
C4-O10-C11	121.649	119.028	118.681	111.675
O10-C11-H16	111.196	111.416	111.595	111.657
O10-C11-H17	111.179	111.386	111.582	106.057
O10-C11-H18	105.645	105.184	105.919	109.207
H16-C11-H17	109.613	109.63	109.27	109.051
H16-C11-H18	109.538	109.535	109.169	109.095
H17-C11-H18	109.585	109.586	109.21	118.4
C1-O12-C30	121.75	119.091	118.753	109.896
C2-C13-H19	109.812	110.1	109.821	108.935
C2-C13-H20	108.896	109.047	108.884	115.006
C2-C13-C21	115.273	115.216	115.268	107.143
H19-C13-H20	107.267	107.323	107.149	107.027
H19-C13-C21	106.86	106.443	106.958	108.54
H20-C13-C21	108.433	108.408	108.453	107.237
C13-C21-H22	107.515	107.157	107.377	112.35
C13-C21-C23	112.788	112.6	112.532	107.752
C13-C21-N27	107.909	107.887	107.719	108.774
H22-C21-C23	108.943	108.989	108.756	106.51
H22-C21-N27	106.788	106.619	106.375	113.86
C23-C21-N27	112.604	113.247	113.723	110.672
C21-C23-H24	110.247	110.3	110.576	110.654
C21-C23-H25	110.619	110.442	110.679	111.737
C21-C23-H26	111.933	111.948	111.753	107.726
H24-C23-H25	107.745	107.806	107.751	107.949
H24-C23-H26	108.063	108.153	107.948	107.952
H25-C23-H26	108.091	108.054	107.984	110.432
H7-H26-C23	97.0435	98.176	110.619	110.191
C21-N27-H28	115.959	113.805	110.455	106.554
C21-N27-H29	115.758	113.459	106.733	111.696
H28-N27-H29	112.717	110.925	111.613	111.605
H12-C30-H31	111.215	111.432	111.525	106.019
O12-C30-H32	111.147	111.33	105.885	109.222
O12-C30-H33	105.607	105.154	109.285	109.071

H31-C30H-32	109.617	109.639	109.189	109.129
H31-C30-H33	109.542	109.56	109.25	110.75
H32-C30-H33	109.627	109.623	110.766	110.851
C9-C34-H35	110.532	110.424	110.743	111.029
C9-C34-H36	110.638	110.714	111.009	108.042
C9-C34-H37	110.987	111.017	108.082	108.021
H35-C34-H36	108.195	108.201	108.091	108.024
C35-C34H-37	108.339	108.303	108.032	108.068
H36-C34-H37	108.048	108.08	108.11	108.126
Dihedral angle(°)				
C6-C1-C2-C3	0.2271	0.2242	-0.324	-0.3673
C6-C1-C2-C13	179.2725	179.7039	-179.731	-179.94
O12-C1-C2-C3	179.6798	79.6527	179.2584	179.155
O12-C1-C2-C13	0.6344	0.173	-0.1483	-0.4175
C2-C1-C6-C5	-0.0646	0.0888	-0.0672	-0.0459
C2-C1-C6-H8	79.6903	79.6153	179.5592	179.6015
O12-C1-C6-C5	179.9649	179.9555	-179.616	-179.53
O12-C1-C6-H8	-0.21	-0.2515	0.0105	0.1171
C2-C1-O12-C30	-174.47	176.1274	-176.683	-176.968
C6-C1-O12-C30	5.4349	3.7459	2.8833	2.5358
C1-C2-C3-C4	0.4012	0.4049	0.4779	0.5127
C1-C2-C3-H7	179.3774	179.394	-179.226	-179.193
C13-C2-C3-C4	179.4455	179.882	179.8833	-179.916
C13-C2-C3-H7	-0.333	0.0831	0.1797	0.379
C1-C2-C13-H19	46.169	46.8291	46.0494	45.665
C1-C2-C13-H20	163.3504	164.332	163.0863	162.7675
C1-C2-C13-C21	-74.5629	-73.5367	-74.8138	-75.1622
C3-C2-C13-H19	-132.842	-132.63	-133.338	-133.894
C3-C2-C13-O20	-15.6605	-15.1274	-16.3009	-16.7915
C3-C2-C13-C21	106.4263	107.0039	105.7989	105.2788
C2-C3-C4-C5	-0.2852	-0.2765	-0.2377	-0.2405
C2-C3-C4-O10	179.8851	179.9045	-179.927	-179.901
H7-C3-C4-C5	179.489	79.5175	179.4591	179.4578
H7-C3-C4-O10	-0.3407	-0.3014	-0.2304	-0.2022
C2-C3-H7-H26	-59.4852	-59.615	-0.1607	-0.1807
C4-C3-H7-H26	120.733	120.584	178.9917	178.8832

C3-C4-C5-C6	-0.0153	-0.0438	179.5522	179.5047
C3-C4-C5-C9	179.3232	79.1222	-1.2955	-1.4314
O10-C4-C5-C6	179.8259	179.7891	1.6901	1.638
O10-C4-C5-C9	-0.8355	-1.0448	-178.011	-178.035
C3-C4-O10-C11	2.3475	2.2294	0.3115	0.3225
C5-C4-O10-C11	-177.489	-177.598	-179.323	-179.333
C4-C5-C6-C1	0.1873	0.2234	-178.842	-178.742
C4-C5-C6-H8	179.5722	179.4874	1.5231	1.6031
C9-C5-C6-C1	179.1517	178.9396	42.3411	41.8907
C9-C5-C6-H8	1.0887	1.3497	158.8045	158.2769
C4-C5-C9-H4	42.0464	43.2342	-79.3545	-79.7956
C4-C5-C9-H15	158.8247	159.9241	-138.532	-139.073
C4-C5-C9-C34	-79.5454	-78.1186	-22.0681	-22.6869
C6-C5-C9-H14	-138.637	137.6302	99.7729	99.2406
C6-C5-C9-H15	-21.8586	-20.9403	60.2666	60.2085
C6-C5-C9-C34	99.7713	101.017	-179.827	-179.875
C3-H7-C6-C23	125.5512	125.2534	-59.8252	-59.7981
C5-C9-C34-H35	60.7348	60.6445	-61.615	-61.5602
C5-C9-C34-H36	-179.438	-179.543	58.2913	58.3561
C5-C9-C34-H37	-59.4996	-59.4932	178.2932	178.4331
H14-C9-C34-H35	-60.9959	-60.9262	-178.216	-178.268
H14-C9-C34-H36	58.8312	58.8861	-58.3095	-58.3518
H14-C9-C34-H37	178.7697	178.9361	61.6924	61.7253
H15-C9-C34-H35	-177.872	-177.625	-62.1885	-62.2328
H15-C9-C34-H36	-58.045	-57.8131	60.3786	60.3644
H15-C9-C34-H37	61.8935	62.237	179.1162	179.088
C4-O10-C11-H16	-62.5093	-62.4929	-63.0582	-63.0069
C4-O10-C11-H17	59.927	60.2695	59.4997	59.5879
C4-O10-C11-H18	178.7322	178.9106	178.2336	178.3013
C1-O12-C30-H31	-64.418	-63.4613	59.2628	59.2119
C1-O12-C30-H32	58.015	59.2837	-60.3804	-60.2541
C1-O12-C30-H33	176.8317	177.9217	173.4756	173.5269
C2-C13-C21-H22	61.3757	60.8094	-63.1458	-63.1723
C2-C13-C21-C23	-58.7462	-59.019	177.211	177.3617
C2-C13-C21-N27	176.2293	175.2768	51.067	51.1427
H19-C13-C21-H22	-60.951	-61.5383	-178.406	-178.505

H19-C13-C21-C23	178.927	178.6333	61.9505	62.029
H19-C13-C21-N27	53.9026	52.9291	-64.1935	-64.19
H20-C13-C21-H22	-176.289	-176.717	179.7739	179.4964
H20-C13-C21-C23	63.5891	63.4547	-60.8983	-61.1621
H20-C13-C21-N27	-61.4353	-62.2495	59.4959	59.1624
C13-C21-C23-H24	-179.219	179.7443	60.9338	60.9309
C13-C21-C23-H25	-60.1479	-61.1871	-179.738	-179.728
C13-C21-C23-H26	60.4624	59.2642	-59.3443	-59.4031
H22-C21-C23-H24	61.4838	60.9816	-57.39	-57.6603
H22-C21-C23-H25	-179.446	-179.95	61.9378	61.6812
H22-C21-C23-H26	-58.8352	-59.4985	-177.668	-177.994
N27-C21-C23-H24	-56.791	-57.5096	-175.142	-175.66
N27-C21-C23-C5	62.2798	61.559	66.9091	66.8902
N27-C21-C23-H26	-177.11	-177.99	-60.2637	-60.8623
C13-C21-N27-H28	-158.498	-165.162	-178.212	-178.312
C13-C21-N27-H29	66.1179	66.742	59.4193	59.0155
H22-C21-N27-H28	-43.1647	-50.3384	-58.5294	-58.4343
H22-C21-N27-H29	-178.549	-178.434	-178.9	-178.879
C23-C21-N27-H28	76.3685	69.5166	68.974	68.982
C23-C21-N27-H29	-59.0159	-58.5792	58.398	58.391
C21-C23-H26-H7	-71.0767	-70.3717	70.692	70.684
24H-C23-H26-H7	167.3395	167.9067	167.256	167.281
H25-C23-H26-H7	50.9918	51.46	51.745	51.698

Table 1: Optimized geometrical parameters for 2,5-Dimethoxy-4-ethylamphetamine computed at HF and DFT [B3LYP] methods with 6-311++G(d,p) basis sets.

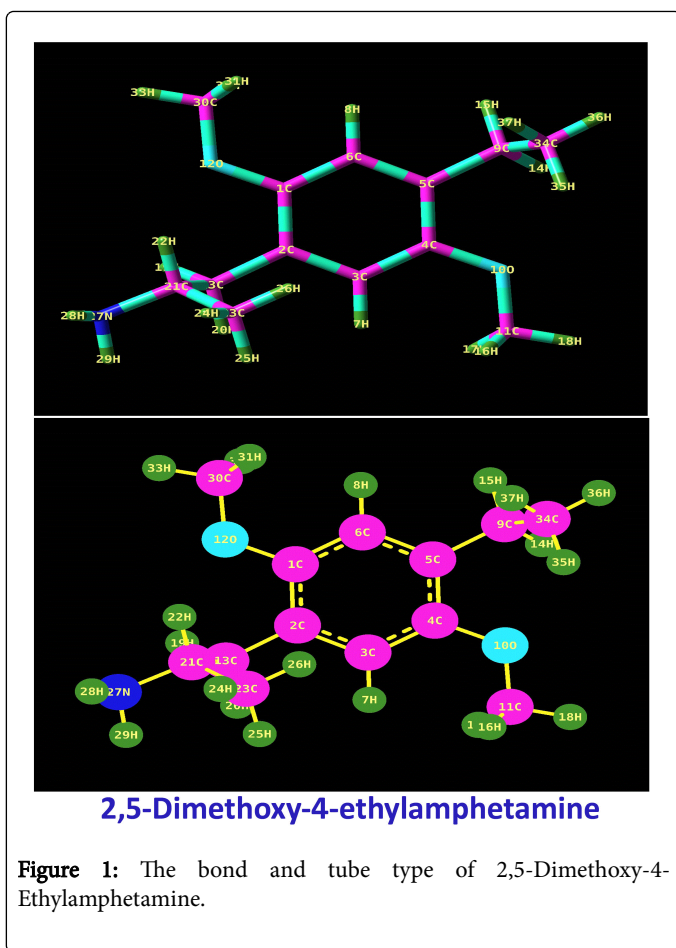
Results and Discussion

Structural deformation analysis

The Molecular Weight of the compound and the Monoisotopic Mass are found to be 223.31 g/mol and 223.15 g/mol respectively. The present compound acting as good inhibitor since the Hydrogen Bond Acceptor Count was 3 and Hydrogen Bond donor was 1. Due to 2 Rotatable Bond Count of the present compound, the molecule possesses five stable conformers with mirror symmetry. Since the Defined and undefined Atom Stereocenter count of the compound were found to be zero and one, the resultant dipole moment was so high. Since the covalently-bonded unit count was unity, the entire bonds were saturated. The rough Complexity of 4-Methoxy-3-methylbenzaldehyde was observed to be 198 which are very high enough to make multi dynamic functions.

The bond and tube type of present compound was displayed in the Figure 1 and the corresponding (111) plane crystal view of thereof

shown in same. The compound under study was basically the derivative of Amphetamine which was composed with couple of methoxy group and ethyl-methyl groups. According to the previous work [11], the bond length between CC of the benzene ring was ranging from 1.392-1.397 Å. In this case, the substituted benzene ring was found to be multi dimensionally broken by the ligand and was evident by the stretching bond length of CC in the range of 1.397-1.404 Å. The entire CC bond length of the ring stretched out and the hexagonal pattern of the ring expanded. The bond length C2-C13 (bond between ring C and amino with ethyl-methyl group chain) was 0.002 Å lesser than C5-C9 (bond between ring C and ethyl-methyl group chain). The bond length limitation was mainly due to the placement of different groups in different dimensions. The ethyl-methyl chain was moved apart from the chain due to the electrochemical polar forces. The symmetrical substitutions of methoxy groups proved their symmetry by the constant bond length; C1-O12=C4=O10=1.403Å.



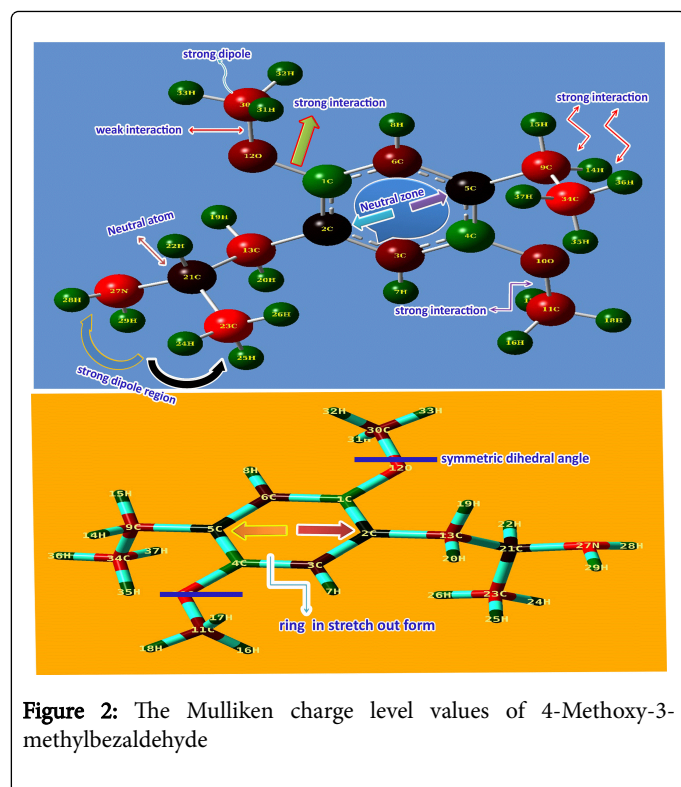
The bond lengths of C-H of the methyl groups were 1.092, 1.092 and 1.085 respectively which are same for that entire methyl group's present compound. This view showed the consistency of methyl groups. The bond angles C1-O12-C30 and C4-O10-C11 were found to same and were equal to 119° and making the R enantiomer which has four times potency in terms of psychedelic activity. The multiple injections of substitutional groups in the base ring showed the resultant molecule in mighty form and renovate the important pharmaceutical phase.

Mulliken charge analysis

The Mulliken charge level values of 4-Methoxy-3-methylbenzaldehyde were displayed in the Table 2 and its diagram was shown in Figure 2. Generally, the charge levels are oriented in carbons (negatively charged) and hydrogen's (positively charged) of the benzene ring without substitutions. When it is substituted, the charges are depleted with respect to the production of the polar and non-polar bonds among the atoms. Thus the charges are reoriented and dynamic chemical potential are generated for inducing the meticulous property. Here, the carbons C2 and C5 in the ring were found to be neutral where the important substitutions were injected whereas at the point of methoxy substitutions, the carbons C1 and C4 are appeared as positive due the sucking of negative charges by O in order to make polar dipoles in methyl group. Rest of two carbons were happened to be negative since there was no ligand. The benzene ring was stretched parallel to the long chain of methyl-ethyl groups.

Atom Position	Charge level
C1	0.25
C2	0.021
C3	-0.144
C4	0.247
C5	0.033
C6	-0.149
C9	0.413
C11	-0.288
C13	-0.375
C21	-0.073
C23	-0.485
C34	-0.504
C30	-0.289
H7	0.168
H8	0.166
H14	0.195
H16	0.18
H17	0.181
H18	0.196
H19	0.205
H20	0.149
H22	0.2
H24	0.157
H25	0.146
H26	0.185
N27	-0.684
H28	0.28
H29	0.272
H31	0.178
H32	0.181
H33	0.198
H35	0.195
H36	0.167
H37	0.167
O12	-0.538
O10	-0.541

Table 2: Mulliken Charges of 2,5-Dimethoxy-4-ethylamphetamine



Dynamic state of charges generate strong dipole moments between the atoms and the substitutions in ortho and meta positions of the universal hexagonal pattern induced special pharmaceutical properties particularly antifungal and anti-biotic properties[12].

Here, two same substituent (methoxy group) were penetrated in ortho and meta positions and made strong dipole moments in the ring which was the main cause of the inducement of the psychedelic activity. There was neutral atom found at midpoint of the CH₂-CH₃-NH₂ chain on meta position of left moiety of ring.

Usually, when the charges are abruptly depleted at a point of atom, a neutral region is formed due to asymmetrical suction of electron cloud. Here, C of CH group was changed as neutral for the creation of strong dipole moment which was also the reason of the incentive of the drug property.

Vibrational analysis

The distinct vibrational fundamental pattern of 2,5-Dimethoxy-4-ethylamphetamine was presented in Table. 3. The scanned FT-IR and FT-Raman vibrational frequencies of observed and simulated spectra by HF and DFT were matched and exhibited in the Figures 3 and 4 respectively. The present novel composite was assembled by two methoxy, two ethyl-methyl group and amino groups with benzene ring. The resultant compound consists of 37 atoms and the structure belongs to CS point group. The 105 fundamental modes of vibrations were dispersed as $\Gamma_{\text{vib}} = 71A' + 34A''$.

S. No.	Symmetry Species CS	Observed frequency(cm ⁻¹)		Calculated frequency			Vibrational Assignments
		FT-IR	FT-Raman	HF	B3LYP	B3PW91	
				6-311++G(d,p)	6-311++G(d,p)	6-311++G(d,p)	
1	A'	3250s	-	3279	3298	3298	(N-H) u
2	A'	3220s	-	3226	3230	3232	(N-H) u
3	A'	-	3080s	3064	3098	3089	(C-H) u
4	A'	-	3050s	3042	3035	3032	(C-H) u
5	A'	-	3030s	3028	3018	3024	(C-H) u
6	A'	-	3010s	3008	3010	3019	(C-H) u
7	A'	2970s	-	2984	2988	2992	(C-H) u
8	A'	2950m	2950s	2948	2987	2995	(C-H) u
9	A'	2940w	2940s	2938	2962	2942	(C-H) u
10	A'	2930w	-	2938	2946	2912	(C-H) u
11	A'	2910m	-	2901	2906	2896	(C-H) u
12	A'	2900m	-	2892	2894	2888	(C-H) u
13	A'	-	2890m	2858	2865	2873	(C-H) u
14	A'	2870w	2870w	2835	2842	2838	(C-H) u
15	A'	2850w	-	2824	2836	2816	(C-H) u

16	A'	-	2840s	2818	2812	2807	(C-H) ν
17	A'	-	2835s	2808	2798	2791	(C-H) ν
18	A'	2830m	-	2802	2788	2789	(C-H) ν
19	A'	2790w	-	2789	2776	2765	(C-H) ν
20	A'	2770w	2770vw	2735	2729	2754	(C-H) ν
21	A'	2740w	2740w	2728	2713	2731	(C-H) ν
22	A'	-	1620s	1632	1625	1618	(N-H) δ
23	A'	-	1600s	1627	1614	1610	(N-H) δ
24	A'	1590s	-	1608	1603	1598	(C=C) ν
25	A'	1560s	-	1580	1569	1562	(C=C) ν
26	A'	1510m	-	1528	1526	1511	(C=C) ν
27	A'	1460m	-	1475	1471	1460	(C-C) ν
28	A'	-	1440s	1466	1498	1482	(C-C) ν
29	A'	1410s	1410s	1421	1426	1421	(C-C) ν
30	A'	1380m	-	1397	1375	1392	(N-H) γ
31	A'	1370m	1370w	1387	1362	1374	(N-H) γ
32	A'	-	1345s	1361	1328	1321	(C-O) ν
33	A'	-	1340s	1338	1315	1312	(C-O) ν
34	A'	-	1305s	1325	1305	1309	(C-H) δ
35	A'	-	1300s	1312	1298	1291	(C-H) δ
36	A'	1250m	1250s	1268	1251	1243	(C-H) δ
37	A'	1240m	-	1269	1243	1221	(C-H) δ
38	A'	1225m	1225s	1236	1212	1209	(C-H) δ
39	A'	-	1220s	1225	1208	1203	(C-H) δ
40	A'	-	1185s	1198	1191	1172	(C-H) δ
41	A'	-	1180s	1187	1174	1158	(C-H) δ
42	A'	1170s	1170vs	1168	1151	1146	(C-H) δ
43	A'	-	1150s	1154	1138	1131	(C-H) δ
44	A'	-	1140s	1135	1123	1118	(C-H) δ
45	A'		1070m	1089	1079	1074	(C-H) δ
46	A'	1040s	-	1069	1059	1035	(C-H) δ
47	A'	990m	-	1003	996	988	(C-H) δ
48	A'	-	980w	993	974	966	(C-H) δ
49	A'	-	970m	987	961	947	(C-H) δ
50	A'	-	960m	978	949	928	(C-H) δ
51	A'	-	940w	958	922	916	(C-H) δ

52	A'	-	920w	933	906	902	(C-H) δ
53	A'	880m	-	901	892	867	(C-N) μ
54	A'	870m	870w	897	872	848	(C-H) μ
55	A'	850m	-	872	848	824	(O-C) μ
56	A'	840m	840w	864	814	807	(O-C) μ
57	A'	-	835s	842	803	799	(C-C) μ
58	A'	830w	830s	838	801	797	(C-C) μ
59	A'	-	825s	832	821	781	(C-C) μ
60	A'	-	820s	825	805	778	(C-C) μ
61	A'	810w	-	822	792	773	(C-C) μ
62	A'	800w	-	787	787	768	(C-H) γ
63	A'	795w	-	781	781	760	(C-H) γ
64	A"	790w	-	753	763	758	(C-H) γ
65	A"	780m	-	824	824	746	(C-H) γ
66	A"	-	760m	726	726	724	(C-H) γ
67	A"	750w	-	780	780	718	(C-H) γ
68	A"	740w	-	766	766	710	(C-H) γ
69	A"	-	730m	755	755	705	(C-H) γ
70	A"	-	720m	711	711	698	(C-H) γ
71	A"	688s	-	702	702	694	(C-H) γ
72	A"	680s	-	686	686	671	(C-H) γ
73	A"	-	645s	646	646	639	(C-H) γ
74	A"	-	640s	634	634	618	(C-H) γ
75	A"	600m	-	605	605	606	(C-H) γ
76	A"	595w	-	578	578	568	(C-H) γ
77	A"	590w	-	567	567	566	(C-H) γ
78	A"	580w	-	582	582	657	(C-H) γ
79	A"	570m	570w	566	556	592	(C-H) γ
80	A"	530w	-	546	586	556	(C-H) γ
81	A"	560w	-	537	577	536	(C-O) δ
82	A"	555w	-	528	519	521	(C-O) δ
83	A'	530w	530w	517	507	513	(C-C-C) δ
84	A'	-	500m	525	498	506	(C-C-C) δ
85	A'	-	460w	470	470	472	(C-C-C) δ
86	A'	-	450w	411	411	443	(C-C-C) γ
87	A'	-	370m	388	388	378	(C-C-C) γ

88	A [*]	-	360m	376	376	365	(C-C-C) γ
89	A [*]	340w	340m	351	351	348	(C-O) γ
90	A [*]	310	-	323	323	314	(C-O) γ
91	A [']	300	300m	234	302	302	(O-C) δ
92	A [']	-	290m	219	288	288	(O-C) δ
93	A [*]	-	250w	213	276	276	(C-N) δ
94	A [']	240w	240vw	202	258	258	(C-C) δ
95	A [']	230w	-	188	238	238	(C-C) δ
96	A [']	210w	-	179	229	229	(C-C) δ
97	A [']	170w	170vw	166	170	170	(C-C) δ
98	A [']	160w	160vw	149	148	148	(C-C) γ
99	A [*]	150w	-	123	134	124	(C-C) γ
100	A [*]	110w	-	73	117	110	(C-C) γ
101	A [*]	100w	100w	68	101	91	(C-C) γ
102	A [*]	90w	-	56	58	68	(C-C) γ
103	A [*]	80w	-	51	54	48	(O-C) τ
104	A [*]	70w	-	42	44	41	(O-C) τ
105	A [*]	50w	-	38	37	37	(C-N) τ

Table 3: Observed and HF and DFT (B3LYP & B3PW91) with 6-31++G(d,p) & 6-311++G(d,p) level Calculated vibrational frequencies of 2,5-Dimethoxy-4-ethylamphetamine.

To get a good correlation with the experimental vibrational modes, it is essential to correct the calculated fundamental frequencies. For this reason, one possible approach involves the rescaling of the force constant matrix, as proposed by Meyer and Pulay [13,14]. The improved procedure has been adopted certainly to improve the agreement between computed and experimental frequencies. However, it was preferable to introduce necessary scaling factors for the fundamental modes was the circuitous approach of scaling the force constants [15]. The HF calculated wave numbers were scaled by the factor 0.910, 0.857 and 0.808, 0.903. The method of B3LYP calculated wavenumbers were scaled by 0.874, 0.933, 0.910 and 0.852 and in the same way B3PW91 were scaled by the factors 0.908, 0.914, 0.852 and 0.879 respectively.

Base ring C-H vibrations: Regularly, the ring and chain complex compound is linked with sustainable ligand tailored fascinated compound for the desired chemical properties. By injecting ligand groups with the base molecule, the vibrational fundamentals might be affected. The impression of interference of ligand group over the base can be measured from the rate of appearance of fundamental pattern of the frequencies and consequently pioneer property of the base compound is altered accordingly. Here, three dissimilar ligand groups were linked with the base compound and by studying the suppression of vibrational pattern of thereof, it can be concluded that, whether the property of the base is changed or not. Accordingly, in general, the C-H stretching vibrations are observed in the region 3000-3100 cm^{-1} for benzene derivatives [16-18]. In this case, the C-H stretching bands

have been found with medium intensity at 3080 and 3050 cm^{-1} in Raman spectrum only. Two vibrations were found within the expected region. This native attitude showed the less influence of ligand on the ring. Here, the C-H in plane and out of plane bending modes were found at 1305 and 1300 cm^{-1} and 800 and 790 cm^{-1} respectively. Usually, those vibrational two different bending bands identified in the region 1300-1000 cm^{-1} and 1000-750 cm^{-1} respectively [19-21]. The in plane bending were pushed well above the expected region whereas out of plane vibrations were pulled down to the lower end of the expected region. Unlike stretching, the bending modes have rather influenced since their strong dipole character of C-H. The entire ring C-H vibrations have not suffered much. This view cleared that, the ring C-H bonds took part in the inducement of new property of the compound.

CC vibrations: Generally, the CC (C=C and C-C) stretching vibrations for phenyl ring are observed in the region 1600 - 1400 cm^{-1} [22-24], in which the wavenumbers in the region 1600 - 1500 cm^{-1} are fundamentally assigned to C=C stretching and the rest to C-C stretching conventionally. In such a case, since C=C and C-C bonds are uncertainty in the ring, three bonds of each to be appeared. Accordingly, the C=C and C-C stretching bands were found at 1590, 1560 & 1510 cm^{-1} and 1460, 1440 & 1410 cm^{-1} respectively. Though the substitutions strongly bonded with the ring and stretched diagonally, the bands related to C=C and C-C stretching were substantially found with strong and medium intensity within the expected region of the spectrum. This appearance depicted the ring enhancement for the compound being with spectacular property. The ring CCC in plane

and out of plane breathing have been found at 460, 450 and 370 cm^{-1} and 360, 340 and 310 cm^{-1} respectively. Even a single ring breathing mode was not been identified within the limit of the observed region. From this condition, it was well known that, due to the loading of different ligand group with huge mass, the ring could not be breathed well.

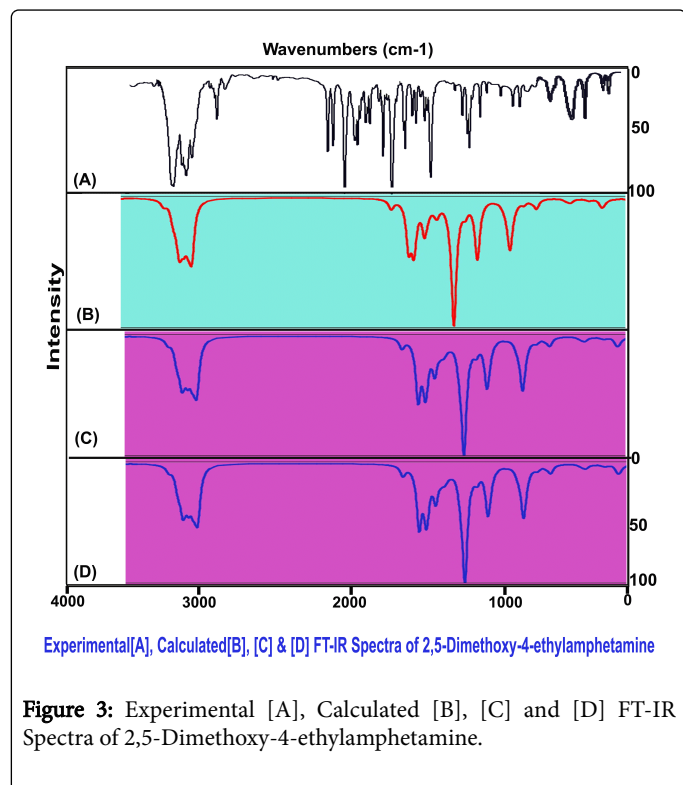


Figure 3: Experimental [A], Calculated [B], [C] and [D] FT-IR Spectra of 2,5-Dimethoxy-4-ethylamphetamine.

Methyl groups vibrations: The substitution of methyl group with the aromatic ring expressed their vibrational frequencies for three; stretching, in plane and out of plane bending vibrations normally taking place in the region of 3000- 2750 cm^{-1} , 1250-950 cm^{-1} and 950-720 cm^{-1} [23, 24] respectively. Accordingly, the stretching vibrational peaks have been identified at 3030, 3010, 2970, 2950, 2940 and 2930 cm^{-1} , in plane bending vibrational peaks were found at 1250, 1240, 1225, 1220, 1185 and 1180 cm^{-1} and out of plane bending signals were found at 780, 760, 750, 740, 730 and 720 cm^{-1} .

All the CH_3 stretching vibrations were located in asymmetric region of methyl group vibrations which represent the enhancement of CH_3 group in the present molecule. Similarly, the bending group of bands; in plane vibrations was observed within the expected region whereas some of out of plane bending modes have appeared below the expected level. Hopefully, such the vibrational impression in the spectrum, explored the certainty that, the methyl group actively participate in the pharmaceutical reactivity.

The methyl group deformation vibrations are very rare to observe and if they are present, the methyl group will be making strong impact on the base structure [25]. Usually, the CH_3 deformation vibrations are expected in the region 1460-1430 cm^{-1} for methyl derivative compounds. But unfortunately, there was no deformation found in the vibrational sequence which was due to the existence of strong dipole moment between C and H.

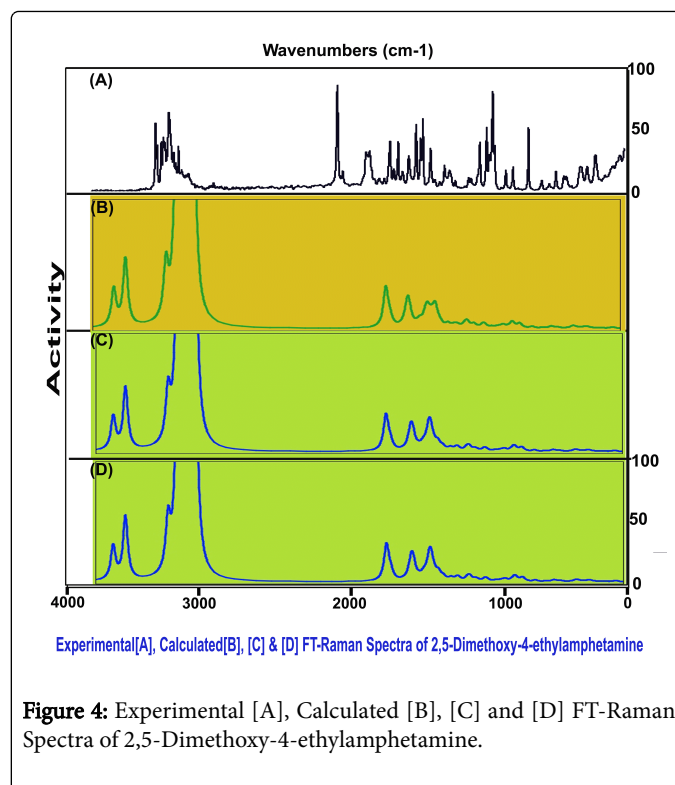


Figure 4: Experimental [A], Calculated [B], [C] and [D] FT-Raman Spectra of 2,5-Dimethoxy-4-ethylamphetamine.

OCH3 vibrations: The methoxy group is compiled with base ring at para position with respect to ethyl-methyl groups which plays the important role in the property of the product. In this case, the electron clouds on O are significantly high and created very weak interaction with C of methyl group. But it forms strong dipole moment with C of ring. Usually, in this condition, strong absorption taking place in IR spectrum. Here, the C-H stretching vibrations appeared with weak intensity at 2910, 2900, 2890, 2870, 2850 and 2840 cm^{-1} . Actually these vibrational region for C-H asymmetric and symmetric stretching is sectioned in the region 2860-2935 cm^{-1} and 2825-2870 cm^{-1} respectively [26, 27]. But, here, most of the stretching belongs to asymmetric and rest of some located in symmetric. Therefore such consistent hike observed in the stretching limit and the above said effect was observed in this case. The in plane and out of plane bending modes were found at 1170, 1150, 1140, 1040, 990 and 980 cm^{-1} and 688, 680, 645, 640, 600 and 595 cm^{-1} respectively. The methoxy derivative compounds have multiple peaks by the absorptions related to C-H in plane and out of plane bending vibrations in the region 1250- 875 cm^{-1} and 850-710 cm^{-1} respectively. In this observation, the considerable impact was found in the out of plane bending absorption bands and this was surely by the asymmetric charge orientation on O.

The C-O and O- CH_3 stretching mode is normally assigned in the region 1350-1300 [28] cm^{-1} and 1100-1000 cm^{-1} respectively for anisole compounds. In this case, the C-O and O- CH_3 stretching vibrations were happened at 1345 & 1340 cm^{-1} and 850 & 840 cm^{-1} respectively. Obviously, the C-O vibrational bands occupied at the top position of well above the expected region whereas the O- CH_3 stretching moved down well below the expected region. This explicit that, the first part have participated in the product property which was found being active. The C-O in plane and out of plane deformations observed at 560 & 555 cm^{-1} and 340 & 310 cm^{-1} respectively. Similarly, the O-C in and out of plane bending modes was found at 300 & 290 cm^{-1} and 80 &

70 cm⁻¹. These bending modes were found at far infrared region and such that the frequencies were also downward due to the rotational effect.

Ethyl group vibrations: The aliphatic C-H stretching bands are expected in the region 3000 - 2900 cm⁻¹ [29,30]. In the present compound the vibrations of the ethyl group are observed at 2830, 2790, 2770 and 2740 cm⁻¹. Similarly, the in-plane and out of-plane deformations of such C-H bond are expected in the regions 1200–1100 cm⁻¹ and 900–700 cm⁻¹ respectively. Four bands due to in-plane and out-of-plane bending are observed at 970, 960, 940 cm⁻¹ and 920 cm⁻¹ and 590, 580, 570 and 530 cm⁻¹ respectively. These observations indicate that, the energy of stretching modes was consumed for the inducement of the new property. Similarly, the in-plane and out-of-plane bending vibrations are moved down from the expected region, because ethylene group acts as bridge between methyl and phenyl ring and it is always affected by either sides of the groups vibrations.

Amino group and C-N vibrations: Generally, the NH group vibrations are very dominative and no way have their vibrational bands not affected. Here the mono amine group was substituted along with the chain of ethyl-methyl group. When the NH group placed between chain and aromatic ring, the secondary N-H stretching vibrational frequencies are observed in the region 3360-3310 cm⁻¹ [31,32]. In this case, the N-H stretching bands were observed at 3250 and 3220 cm⁻¹. The in plane and out of plane bending signals have appeared at 1620 & 1600 cm⁻¹ and 1380 & 1370 cm⁻¹ respectively. The N-H in plane and out of plane bending are expected in the range 1490-1580 cm⁻¹ and 900-700 cm⁻¹ [33,34] respectively. In this case, the stretching vibrations were moved down well below the expected region where as in plane and out of plane bending bands moved up extremely well above the expected region. Due to the favouring of charge levels in amino group, the bending mode only were active. The C-N stretching vibrations, in plane bending and out of plane bending vibrations are generally observed in the region 1155-1130 cm⁻¹, 550-400 cm⁻¹ and 400-360 cm⁻¹ respectively [35,36]. In this title compound, the C-N stretching, in plane and out of plane bending bands were observed at 880, 250 and 50 cm⁻¹ respectively. These vibrations were affected much due to the less energy availability and moved in far infrared region.

NMR Analysis

The paramagnetic shield of group of atoms is broken by the attainment of bonding. The chemical properties are alternatively changed with respected to the dynamic character of the electron cloud. Thus the chemical property is exchanged and modified according to the electronic charge transformation. Similarly, the molecule is formed by making bonds with substitutional groups. Therefore corresponding chemical property of the product-compound is complicated and which depends upon their asymmetrical displacement of electron clouds [11]. The change of chemical property is scaled by the chemical shift of associated atoms.

The computed values in gas and solvent phase, along with the experimental values are presented in the Table 4 and the experimental spectra are presented in Figure 5. The aromatic carbon atoms generally [37] have shifts in the range of 120-130 ppm. In the present compound the chemical shifts of the aliphatic carbon atoms C9, C11, C13, C21, C23, C30 and C34 were ranging from 11-55 ppm. But, the carbons of the aromatic ring; C1-C6 were lie in the range of 115-159 ppm experimentally and between 121-161 ppm theoretically. In the case of C3 and C6, there was no substitutional group found, the chemical shift was found to be 115 and 128 ppm respectively. But, the rest of others

have large shift which was purely due to the asymmetrical breaking of the paramagnetic shield of the particular carbon. The chemical shift of C1 and C4 was so high which was mainly due to the energy transformation from methoxy group via ring. The transferred energy was exchanged between ring and ethyl-methyl groups. Due to this transformation, the particular carbon in the ring appeared to be neutral. Such a condition shows that, the inherent change of property of the benzene ring in this compound. This trend is in accordance with the charge predicted by Mullikan analysis.

Atom position	Chemical Shift - TMS-B3LYP/6-311G(2d,p)			Experimental shift (ppm)
	Gas	Solvent phase		
		DMSO	Chloroform	
C1	158.9	157.99	158.28	159.5
C2	131.742	132.49	132.31	128.5
C3	127.77	129.28	128.75	129
C4	161.67	161.67	161.69	159.5
C5	136.46	136.11	136.2	130
C6	122.33	121.73	121.91	115
C9	20.77	20.46	20.55	15
C11	49.67	50.42	50.18	40
C13	25.3	24.81	24.96	15
C21	45.21	44.77	44.89	54.5
C23	34.69	34.01	53.67	38
C30	53.32	53.81	53.67	55
C34	8.35	8.2	8.24	11
H7	12.6	12.98	12.87	9.6
H8	5.8	5.92	5.88	7.2
H14	1.59	1.46	1.51	1.5
H15	0.57	0.65	0.61	-
H16	2.5	2.75	2.68	-
H17	1.7	1.93	1.89	1.2
H18	2.42	2.59	2.56	2.7
H19	1.74	1.53	1.61	-
H20	0.26	0.36	0.33	-
H22	1.27	1.34	1.32	-
H24	0	0.21	0.14	-
H25	0.64	0.4	0.48	-
H26	7.8	7.5	7.61	7.2
H28	0.84	0.55	0.64	-
H29	0.74	1	1.08	-

H31	2	2.21	2.18	-
H32	2	2.16	2.11	-
H33	2.4	2.54	2.56	-
H35	0.25	0.39	0.3	-
H36	0.25	0.27	0.487	-
H37	0.63	0.53	0.57	-

Table 4: Experimental and calculated ¹H and ¹³C NMR chemical shift in 2,5-Dimethoxy-4-ethylamphetamine.

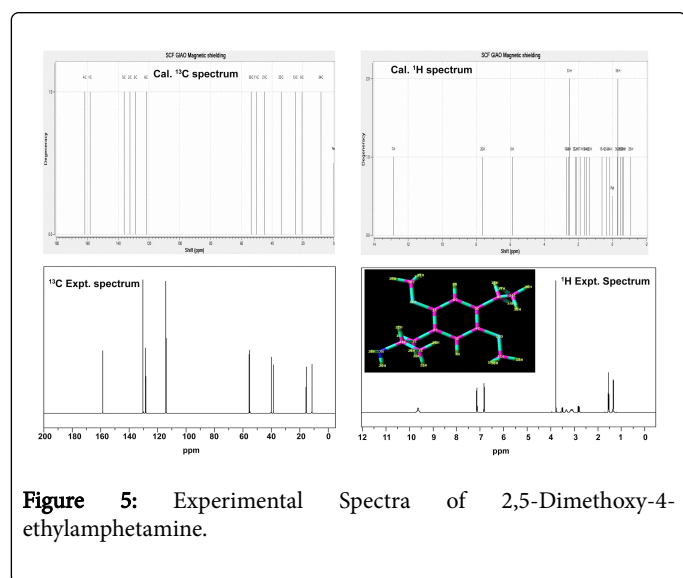


Figure 5: Experimental Spectra of 2,5-Dimethoxy-4-ethylamphetamine.

The chemical shift of carbon atoms C13 and C34 in the ethyl and methyl groups has of 15 and 11 ppm experimentally and 24 and 8 ppm theoretically, these were lower than the expected values. When the negative charge domain is dislocated towards the CH and NH₂ groups, the negative charges were exchanged via C13 and made as virtually shielded and neutral.

So, the chemical shift of such carbon becomes very low and below 50 ppm. In the case of C34, the charges were moved asymmetrically to the ethyl group and making strong dipole. The chemical shift of C21 was found to be 54.5 ppm and made as neutral which was due to the absorption of charges by the amino group.

In this case, the chemical shift value was rather increased which was clearly due to the presence of four σ bond character.

The chemical shifts of the hydrogen atoms in benzene ring as well as methyl group are expected between 7-8 ppm. In this case, ring related hydrogen's H7 and H8, the chemical shift was found to be within the limit at both experimentally and theoretically.

The entire H of alkyl, ethyl and methyl groups were found to be very low and some of the chemical shift was not observed. This view showed the charge prediction by Mullikan analysis for hydrogen atoms are correct. Except H7 and H8, the entire theoretical shift was found to be 0.5 - 2.0 ppm and this trend is in tune with the above literature.

There was no appreciable difference observed in the chemical shifts in different solvents phases. Hence the impact of the solvents on the chemical shifts of the compound for various atoms is negligibly small.

Frontier molecular interaction profile

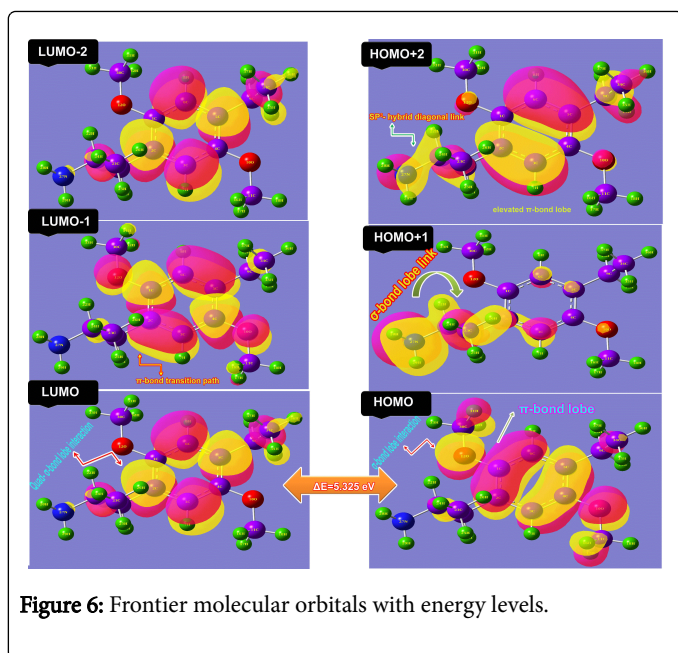
After the assembly of molecular orbitals in the compound, the charge depletion region is formed generally between two elevated orbitals with different characteristics called HOMO and LUMO.

Such these orbitals are arranged with respect to the energy of bonded molecules and some the orbitals with same energy are usually overlapped with one another and intersected. The overlapped orbitals are shared by the electrons and they spent most of the time on blended orbitals separately in HOMO and LUMO.

The transitions taking place between those orbitals strongly set the chemical character of the compound and thus, the new physico-chemical property was induced in the compound. The energy of Frontier molecular structure was depicted in the Table 5 and the diagram was displayed in Figure 6.

Energy levels	IR region	UV-Visible region
	B3LYP/ 6311G Energy (eV)	B3LYP/ 6311G Energy (eV)
H+10	-9.8918	-9.599
H+9	-9.6056	-9.469
H+8	-9.4709	-9.469
H+7	-9.1615	-9.1503
H+6	-9.0983	-9.0298
H+5	-9.0586	-8.2932
H+4	-8.799	-7.9593
H+3	-8.43	-7.3073
H+2	-7.731	-6.7925
H+1	-6.6733	-6.2474
H	-5.8675	-6.0597
L	-0.117	-0.3333
L-1	0.4764	0.0712
L-2	1.203	0.9455
L-3	1.3344	1.3698
L-4	1.6593	1.4645
L-5	1.9243	1.7567
L-6	2.2389	1.8569
L-7	2.382	1.9763
L-8	2.2389	2.415
L-9	2.382	2.5959
L-10	2.4558	2.6332

Table 5: Frontier molecular orbitals with energy levels.



Here, in HOMO, the right and left moiety (CCC semi-circle) of the ring system occupied by π -bond overlapping whereas methoxy group making δ -bond overlapping with O. There was no electron occupied orbitals found on ethyl and methyl groups' and also there was no orbital interaction lobes were found on same system. In the case of LUMO, σ -bonding overlapping was appeared on the C-C and C-H of the ring and another σ -bond overlapping lobes were occupied over ring ethyl and methyl group whereas the methoxy groups were abandoned. From this view, it was clear that, the electron density were reoriented asymmetrically and they were prepared to provide the charges to the LUMO to induce chemical energy for generating psychotogenic character. In addition to that, HOMO+1, σ -bond lobes in cascade form were found at amino-ethyl-methyl chain group and some of the orbital interaction residue was observed over the ring carbons and methoxy groups. From this view, the chemical energy was started from this group and transferred via C of the ring. In the case of HOMO+2, there were strong π and δ -bond overlapping lobes identified over the ring carbons and two ethyl-methyl chains. From this view, it was observed that, the energy was exchanged between two chains via ring. There were no other lobes over rest of the atoms. In LUMO-1, two π -bond and three σ -bond overlapping of orbitals were to be appeared in ring and methoxy group while in the case of LUMO-2, only σ -bonded lobes were found in the ring. Form this display of orbital lobes; it was obvious that, in HOMO spatial quantization, the aggressive δ -bonding donor orbitals were available for supplying the

chemical energy over the empty orbitals whereas in LUMO sequence, σ and π bonding lobes appeared on ring and ligand groups. This arrangement was suitable for creating the drug for treating hyperactivity disorder. For forming potential drug, the chemical energy transition was restricted among the orbitals by 5.325 eV which was very high and enough to sustain the property. The energy values of frontier molecular levels were presented in the Table 5.

UV-visible absorption analysis

The confinement of vibrational energy states depends on the impact of the ligand groups on the base molecule. The energy was supposed to be within the transition among the energy states which shift the vibrational pattern (wavenumber region) of the resultant compound from lower to higher or vice versa. Thus the electronic shift also is observed in the electronic energy states pattern. A charge transfer complex or electron donor-acceptor complex is associated with different energy domain of the molecule, in which electronic charges are transferred between the two entities of molecule. The resulting electrostatic attraction provides a stabilizing force for the molecular complex. The charge transfer is taking place anywhere in the molecular complex and usually, the electronic transition is occur into an excited electronic states of the substitutional group and among different parts of the base molecule. These electronic transitions into the coordinated excited electronic states of different entities of the compound frequently occur in UV-Visible region which characterize the physical and chemical property.

In this case, the electronic excitation absorption CT band was found at 250 nm of oscillator strength 0.05 on the energy gap of 4.95 eV and was assigned to $n \rightarrow \pi^*$ in gas phase. The energy of CT complex was found to be 4.95 eV is enough to make sure the transition between acceptor (ethyl-methyl-amino group) and donor (phenyl ring) whereas the observed UV-Visible band was identified at 260 nm. The experimental CT band was shifted to higher wavelength region since the source material was in solid phase. In solvent phase, the CT band is identified at 249 nm with oscillator strength of 0.07 at the same energy gap. The attained result of CT complex in gas as well as solvent phase showed the strong interaction between donor (methoxy) and acceptor (phenyl). The absorption band of present compound was transparently occurring in the UV spectrum in R-band (German, radikalartig) and consistently being with anti-depression activity. In this case, the identification of absorption band in quartz-UV region predicted that, the symmetrical placement of methoxy entities in opposite sides of the ring was playing the important role of such pharmaceutical action. The electronic excitation parameters are presented in the Table 6 and the absorption band was displayed in the Figure 7.

λ (nm)	E (eV)	(f)	Major contribution	Assignment	Region	Bands
Gas						
250.38	4.9519	0.0562	H@L (92%)	$n \rightarrow \pi^*$	Quartz-UV	R-band (German, radikalartig)
235.5	5.2647	0.0003	H@L (89%)	$n \rightarrow \pi^*$		
219.55	5.6472	0.0201	H@L (86%)	$n \rightarrow \pi^*$		
DMSO						

249.61	4.9671	0.0704	H@L (90%)	$n \rightarrow \pi^*$	Quartz-UV	R-band (German, radikalartig)
236.95	5.2326	0.0002	H@L (90%)	$n \rightarrow \pi^*$		
221.64	5.5939	0.015	H@L (87%)	$n \rightarrow \pi^*$		
Chloroform						
250.13	4.9568	0.074	H@L (86%)	$n \rightarrow \pi^*$	Quartz-UV	R-band (German, radikalartig)
236.38	5.2452	0.0003	H@L (85%)	$n \rightarrow \pi^*$		
220.84	5.6142	0.0207	H@L (78%)	$n \rightarrow \pi^*$		

Table 6: Theoretical electronic absorption spectra of 2,5-Dimethoxy-4-ethylamphetamine (absorption wavelength λ (nm), excitation energies E (eV) and oscillator strengths (f)) using TD-DFT/B3LYP/6-311Gmethod.

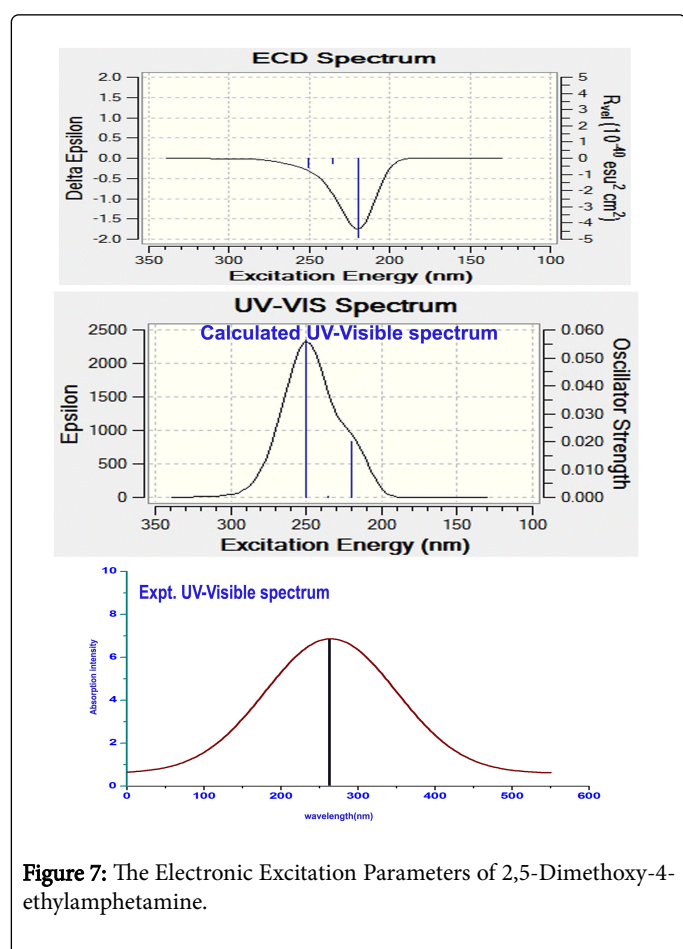


Figure 7: The Electronic Excitation Parameters of 2,5-Dimethoxy-4-ethylamphetamine.

The rearrangement of electronic orbitals on par with the equilibrium force of attraction existing between the dipoles of the compound induced the local electric field which making instantaneous polarization causing ECD.

The interaction of chromophores and auxochrome with base compound providing smaller energy increments for transition to excited states modify the chemical activity of the compound which can be identified in the ECD spectra. As in the Figure 7, the ECD absorption band was identified at 220 nm which was nearly equal

energy absorption as UV-visible energy transition. This effect explored the unique chemical reactivity.

Molecular Electrostatic Potential (MEP) maps

The asymmetrical charge reorientation of the molecule has been organized by the restoring chemical equilibrium forces from the arrangement of different dipoles in various part of the compound.

Such an elevated charge orientation over the molecule was produced by homo and hetero nuclear bonds of the ring and ligand groups.

Here, the main frame of molecule was substituted by three dissimilar atomic groups and thereby the asymmetric charge orientation causing strong electrostatic potential between two extreme charge levels. The electrostatic appearance among various parts of the molecule was shown in the Figure 8.

The faded electron rich and electron deficient zones were distinguished by the red to blue colour region on the molecule. The electron rich showed intensive red and proton wealthy part identified by concentrated blue.

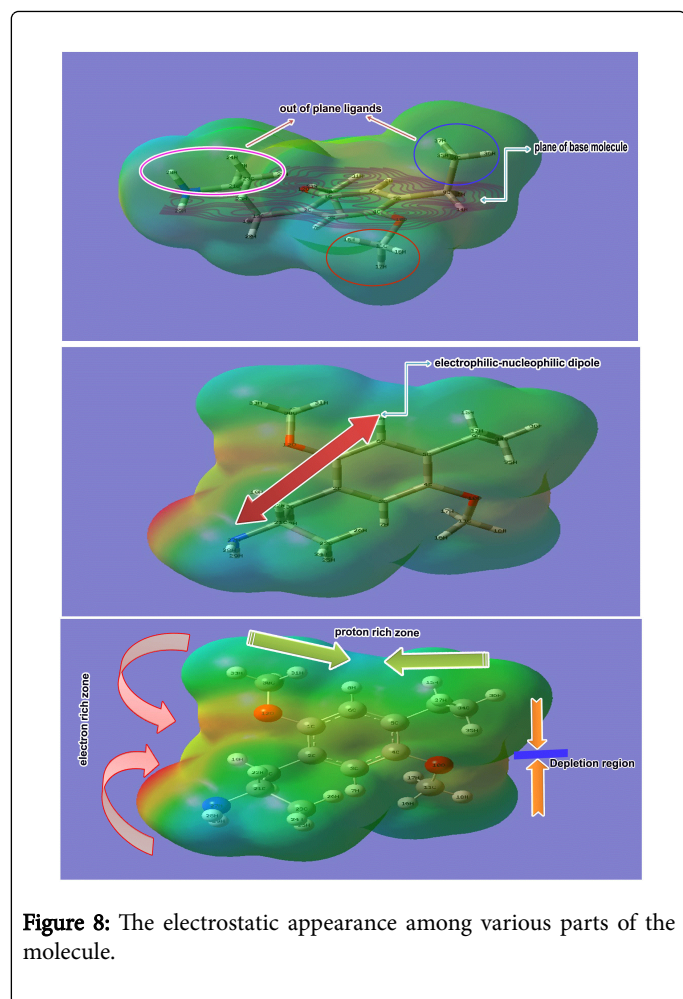
In the Figure 8, the electron bustle zone was captured over the O of methoxy group and N of amino group. The moderate negative region was concealed over the ring carbons and further decayed when moved towards chain.

The protonic content was incarcerated on the hydrogen zones over the methyl group. It was copious in around the edge of the molecule and deficient in carbon bonded side. This faze situation was induced by the hydrogen bond chaos on methoxy and methyl groups.

Due to the electron pulling away from the ring, the electrostatic energy was found to be uniform at the centre part of the ring and acted as defect free energy grid. In each and every molecule has strong ligand which is the root cause of the major property of the compound.

In this case, the strong electrophilic-nucleophilic dipole was found between ring C-H and N of amino group and o of methoxy group. The out of plane ligand usually making strong receptor activity when docking is made.

Here, methoxy and ethyl-methyl chain appeared as out of plane ligand which was indicated in the Figure 7.



Polarizability and hyperpolarizability analysis

The chemical force of attraction stabilized the polarized orbitals in different coordinates of the molecule which facilitate the strong physico-chemical property and can be measured by computing Polarizability and first order hyperpolarizability as in the Table 7.

The calculated value of the dipole moment was found to be very less (0.935 Debye) since the multi pole moments were found to be dispersed in different dimensions. The ligand in the compound oriented in different sides and the resultant dipole moment was very low. The calculated showed that, the major entities were found to be on x and y coordinates of the compound which point out the direction of the chain and methoxy group.

The calculated average polarizability and anisotropy of the polarizability is 198×10^{-30} esu and 268×10^{-30} esu, respectively. The hyperpolarizability β is one of the important key factors of stabilization of frontier molecular orbital interaction system. The B3LYP/6-311++G(d,p) calculated first hyperpolarizability value (β) is 187.7×10^{-33} esu. From this observation, it was clear that, the hyper asymmetrical polarization was taking place abruptly to empower the frontier molecular orbitals for the stimulation of pharmaceutical property.

Parameter	a.u.	Parameter	a.u.
α_{xx}	-102.4282	β_{xxx}	-15.8134
α_{xy}	0.2259	β_{xxy}	-20.5931
α_{yy}	-79.5913	β_{xyy}	-2.9661
α_{xz}	-5.8184	β_{yyy}	8.6568
α_{yz}	2.4708	β_{xxz}	26.1358
α_{zz}	-102.6729	β_{xyz}	2.1077
α_{tot}	198.432	β_{yyz}	-11.5149
$\Delta\alpha$	268.436	β_{xzz}	-4.7675
μ_x	0.1763	β_{yzz}	-0.9354
μ_y	-0.4912	β_{zzz}	-1.493
μ_z	0.7768	β_{tot}	187.7
$\Delta\mu$	0.9358		

Table 7: The dipole moments μ (D), the polarizability α (a.u.), the average polarizability α_0 (esu), the anisotropy of the polarizability $\Delta\alpha$ (esu), and the first hyperpolarizability β (esu) of 2,5-Dimethoxy-4-ethylamphetamine.

Thermodynamical functions analysis

Normally, the thermo dynamical analysis on aromatic compound is very important since they provide the necessary information regarding the chemical reactivity [12]. The thermodynamic functional parameters were depicted in the Table 8. The variation of thermodynamic functional parameters with temperature was shown in Table 8. The calculated entropy, specific heat capacity and enthalpy were found to be varied with positive temperature coefficient. When the temperature increased from 100K to absolute temperature 298.15, the functional parameters were varied unhurriedly whereas from 350 to 1000K, the thermodynamical functions established to swing as linear pattern and rather constant at maximum temperature. This view of variation showed the consistent chemical reactivity and considerable chemical hardness of the present compound. The Gibbs free energy is always negative temperature coefficient and here, since it was found to be true, the present compound has strong and unique chemical property and endless chemical reaction.

T(K)	(cal mol ⁻¹ K ⁻¹)	(calmol ⁻¹ K ⁻¹)	(kcalmol ⁻¹)	Gibbs free energy $\Delta G = \Delta H - T\Delta S$ KJmol ⁻¹
100	359.47	132.87	8.09	-35938.9
200	477.67	214.28	25.61	-95508.4
298.15	577.18	289.86	50.32	-172036
300	578.98	291.32	50.85	-173643
400	673.54	369.21	83.91	-269332
500	763.7	439.82	124.44	-381726
600	849.36	500.04	171.52	-509444

700	930.36	550.72	224.13	-651028
800	1006.78	593.58	281.41	-805143
900	1078.86	630.1	342.64	-970631
1000	1146.91	661.42	407.25	-1146503

NBO transition analysis

The NBO data of the compound was derived from perturbed and non-perturbed frontier molecular orbitals in which the electronic energy was exchanged. The energy was transferred among various energy domains for standardize the significant orbitals for obtaining desired physical and chemical characteristics [38]. In this venture, the donor and acceptors of electronic orbitals were identified and their energy transitions were tabulated in Table 9.

Table 8: Thermodynamic parameters at different Temperatures for 2,5-Dimethoxy-4-ethylamphetamine.

Donor [i]	Type of bond	Occupancy	Acceptor [j]	Type of bond	E2 [kcal/mol]	Ej – Ei [au]	F(i j) [au]
C1-C2	σ	1.97172	C2-C3	σ^*	3.39	1.28	0.059
C1-C2	σ	1.97172	C3-C4	σ^*	19.39	0.28	0.066
C1-C2	σ	1.97172	C5-C6	σ^*	19.43	0.29	0.067
C1-C6	π	1.976	C1-C2	π^*	4.57	1.28	0.068
C1-C6	π	1.976	C2-C13	π^*	3.4	1.1	0.055
C1-C6	π	1.976	C5-C6	π^*	3.52	1.28	0.06
C2-C3	π	1.96654	C1-C2	π^*	3.61	1.27	0.061
C2-C3	π	1.96654	C1-O12	π^*	4.19	0.98	0.057
C2-C3	π	1.96654	C3-C4	π^*	3.59	1.25	0.06
C2-C3	π	1.96654	C4-O10	π^*	4.04	0.98	0.056
C2-C13	σ	1.97109	C1-C6	σ^*	3.26	1.15	0.055
C3-C4	σ	1.67521	C2-C3	σ^*	3.65	1.28	0.061
C3-C4	σ	1.67521	C2-C13	σ^*	3.27	1.1	0.054
C3-C4	σ	1.67521	C4-C5	σ^*	4.6	1.28	0.069
C3-C4	σ	1.67521	C5-C9	σ^*	3.22	1.1	1.1
C3-C4	σ	1.67521	C1-C2	σ^*	20.49	0.29	0.07
C3-C4	σ	1.67521	C5-C6	σ^*	20.92	0.29	0.071
C3-H7	σ	1.97462	C1-C2	σ^*	4.27	1.11	0.061
C3-H7	σ	1.97462	C4-C5	σ^*	3.76	1.11	0.058
C4-C5	π	1.97208	C3-C4	π^*	4.32	1.26	0.066
C4-C5	π	1.97208	C5-C6	σ^*	3.2	1.29	0.057
C5-C6	σ	1.96709	C1-C6	σ^*	3.44	1.25	0.059
C5-C6	σ	1.96709	C1-O12	σ^*	4.06	0.98	0.056
C5-C6	σ	1.96709	C1-C2	σ^*	20.34	0.29	0.069
C5-C6	σ	1.96709	C3-C4	σ^*	19.38	0.28	0.067
C5-C9	σ	1.97355	C3-C4	σ^*	3.31	1.15	0.055
C6-H8	σ	1.97461	C1-C2	σ^*	3.78	1.11	0.058
C6-H8	σ	1.97461	C4-C5	σ^*	4.24	1.11	0.061
C9-H14	σ	1.97872	C5-C6	σ^*	3.27	1.08	0.053
C9-H15	σ	1.98004	C4-C5	σ^*	3.01	1.07	0.051

C13-H19	σ	1.97768	C21-C23	σ^*	3.32	1.07	0.053
C23-H26	σ	1.98554	C21-N27	σ^*	3.48	0.86	0.049
O10	n	1.9678	C3-C4	σ^*	4.67	1.14	0.065
O10	n	1.9678	C3-C4	σ^*	17.03	0.34	0.073
O10	n	1.9678	C11-H16	σ^*	4.52	0.72	0.052
O10	n	1.9678	C11-H17	σ^*	5.67	0.72	0.058
O12	n	1.96751	C1-C6	π^*	4.65	1.14	0.065
O12	n	1.96751	C1-C12	π^*	16.37	0.35	0.073
O12	n	1.96751	C30-H31	σ^*	4.5	0.72	0.052
O12	n	1.96751	C30-H32	σ^*	5.67	0.72	0.058
N27	n	1.96142	C23-H26	σ^*	6.81	0.68	0.061
C3-C4	σ	0.02637	C1-C2	σ^*	316.66	0.01	0.082

Table 9: The calculated NBO of 2,5-Dimethoxy-4-ethylamphetamine by second order Perturbation theory.

Usually, the electron density delocalized among occupied Lewis type (bond or lone pair) orbitals and unoccupied (anti-bonding and Rydberg) non-Lewis orbital in order to stabilize donor acceptor interaction [39]. Here, in ring system, the transition from C1-C2 to C3-C4 and C5-C6 and they assigned to $\sigma\text{-}\sigma^*$ in which 19.39 kcal/mol energy was transferred from first chain to second chain in order to connect the major ligand groups. In same system, another transitions from C3-C4 to C1-C2 and C5-C6 which were assigned to $\sigma\text{-}\sigma^*$ with energy of 20.50 kcal/mol respectively. In these transitions, the received energy was exchanged from methoxy group to chain and another methoxy group on another side. Similarly, the transitions were taking place from C5-C6 to C1-C2 and C3-C4 by $\sigma\text{-}\sigma^*$ interaction with the energy of 20.3 and 19.3 kcal/mol respectively. In this case, the energy was transferred in order to blend the Lewis of chain and methoxy group. It was very rare to take place the transitions from lone pair to other system. Here it was happened from C5-C6 to C1-C2 and C3-C4 with the exchanged energies of 20.3 and 19.3 kcal/mol respectively for the back donation of interaction energy (from chain to methoxy group). The huge amount of energy of 316.6 kcal/mol was transferred from C3-C4 to C1-C2 for the two symmetrical chain and methoxy groups. In these transitions, the electronic energies exchanged between ligand to ligand via the ring and also the residue energy was transferred from the chain to the ring system. Thus the energy was exchanged back and forth among the orbitals to make desirable physical and chemical property of the study compound.

Physico-chemical properties

The chemical properties and molecular reactivity descriptors of the present compound were computed from Frontier molecular energy levels. The entire parameters were presented in the Table 10. The resultant dipole moment is the measuring scale of asymmetric charge orientation of compound and the Total determined dipole moment was found to be 0.93 and 2.34 dyne in IR and UV-visible region respectively. In this case, the base compound is benzene; its dipole moment is almost zero. Here, the total compound composed by multiple ligands with benzene ring. Due to the symmetrical substitutions in ortho and meta positions in the ring, the total

computed dipole moment was found to be very low and it ensured that symmetric charge orientation for the desired pharmaceutical property. The energy gap of the frontier molecular orbitals measured usually, the chemical stability of the compound; the same was determined to be 2.66 and 2.86 eV in IR and UV-Visible region respectively. Both the values showed moderate chemical stability and also it was appeared in non-reactive Quartz UV region.

Parameter	B3LYP 6311G	UV-Visible	Electrophilicity charge transfer (ECT) (ΔN_{max})A-(ΔN_{max})B
Etotal (Hartree)	7.13	-7.13	1.321
EHOMO (eV)	5.442	6.059	
ELUMO (eV)	0.117	0.333	
$\Delta E_{H\cong M\cong -\Lambda Y M\cong \gamma\pi\pi}$ ($\epsilon\zeta$)	5.325	5.726	
EHOMO-1 (eV)	6.343	6.13	
ELUMO+1 (eV)	6.556	6.58	
$\Delta E_{H\cong M\cong -1-\Lambda Y M\cong +1\gamma\pi\pi}$ ($\epsilon\zeta$)	12.9	0.449	
Chemical hardness (h)	2.662	2.863	
Electronegativity (χ)	2.662	2.863	
Chemical potential (μ)	2.662	2.863	
Chemical softness(S)	10.65	11.452	
Electrophilicity index (ω)	1.331	1.431	
Dipole moment	0.935	2.34	

Table 10: Calculated energies, chemical hardness, electro negativity, Chemical potential, Electrophilicity index of 2,5-Dimethoxy-4-ethylamphetamine.

The electron affinity of the molecule is very important for the determination of the reaction ability of receptor protein and was found to be 5.44 which were elevated to the extreme and the reaction capability of the present compound is energetic. The ionization potential of the compound is significant to evaluate chemical-bond reorganization. The ionization potential was found to be 0.11 which is very small and was main reason for the low dipole moment and it was enough to maintain the chemical bond stability. Generally, the chemical hardness is a scale of obstacle for transformation of charge whereas the electronegativity is measure of the tendency to attract electrons by inter-chemical bond [39]. Here, both parameters were found to be 2.66 which was moderate and illustrated the good reactive character and it was not possible to add further additive drug properties.

The electrophilicity index is an indicator of energy flow via frontier molecular orbitals. In this case, the electrophilicity index was recognized to be 1.331 eV, but the same was 2.09 eV for benzene ring. The derived energy was very low due to the symmetrical existence of the ligand groups. From this point of view, it was clear that, the maximum energy exchanged between ligand via ring for creating the prosperous pharmaceutical application. Here, the benzene acted as base compound and it was substituted with ethyl-methyl-amino groups and methoxy groups in balanced form and the electrophilicity charge transfer of the compound was found to be + 1.321 which emphasized the maximum charge flow from ligand to ligand via benzene. This also major reason for the present compound is an anti-depression agent.

VCD verification

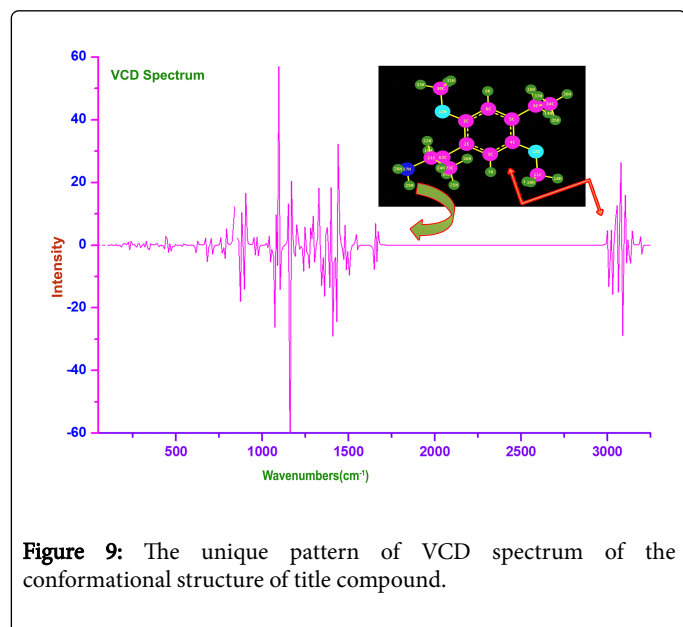


Figure 9: The unique pattern of VCD spectrum of the conformational structure of title compound.

The good Chirality of the compound can have good biological and pharmaceutical property with hiding of toxicity. The architecture of the chirality reflects masking of side effect. The regular peak sequence on both sides was created by circularly polarized infrared radiation during a vibrational transition. Generally, the peaks are found to be in unique sequential pattern. In addition to that, there were few small opaque parts identified in different region of the spectrum which reflect the unwanted properties. This is mainly due to the flaw in optimization which can be removed by re optimizing the structure. The unique

pattern of VCD spectrum of the conformational structure of title compound was displayed in the Figure 9. The VCD of present compound showed the R- enantiomer and emphasized the optical and chemical purity of the present substance.

Conclusion

The present compound; 2,5-Dimethoxy-4-ethylamphetamine was the primary derivative of Amphetamine. In order to evaluate and determining unknown properties, the basic Amphetamine was substituted by suitable ligand and different analyses have been made on the chemical structure. The molecular deformation analysis gave the complete information regarding the structure activity on par with the ligand. The charge reorientation among bonded entities revealed the asymmetric movement of the charges which was favoured for inducement of peculiar drug property. The vibrational assignments of the compound explicit the fundamental IR and Raman frequencies which were consistently emphasized the correct compositional bonds which composed the compound. The chemical reaction path arrangement of different carbons was ensured from the discrete chemical shift and the background reason was extracted. The orbital interaction lobe formation favoured for the chemical process to produce desirable drug property was predicted from the cascade arrangement of HOMO-LUMO. The chromophores reactivity on the base compound causing the electronic shift in UV-Visible spectra was discussed in detail. The electronic energy transition from donor and acceptor orbitals was studied. The consumption of energy between ligand and base compound was measured and maximum energy flow among the orbitals for the completion of the drug property was determined.

Conflict of Interest

As a corresponding Author, I hereby declare that there is no conflict with other fields and other persons belong to field.

References

1. Snyder SH, Faillace LA, Weingartner H (1969) A new psychotropic agent. *Arch Gen Psychiatry*. 21: 95-101.
2. Weingartner H, Snyder SH, Faillace LA, Markley H (1970) Altered free associations: Some cognitive effects of DOET (2, 5-dimethoxy-4-ethylamphetamine). *Behav Sci* 15: 297-303.
3. Snyder SH, Weingartner H, Faillace LA (1971) DOET (2, 5-dimethoxy-4-ethylamphetamine), a new psychotropic drug: Effects of varying doses in man. *Arch Gen Psychiatry* 24: 50-55.
4. Heal DJ, Smith SL, Gosden J, Nutt DJ (2013) Amphetamine, past and present—a pharmacological and clinical perspective. *J Psychopharmacol* 27: 479-496.
5. Adderall XR (2013) Prescribing Information, United States Food and Drug Administration. Shire US Inc. 12-13.
6. In Sydor A, Brown RY (2009) *Molecular neuropharmacology: A foundation for clinical neuroscience* (2nd ed.) McGraw-Hill Medical, New York. 367.
7. Moorthy N, Prabakar PJ, Ramalingam S, Pandian GV, Anbusrinivasan P (2016) Vibrational, NMR and UV-visible spectroscopic investigation and NLO studies on benzaldehyde thiosemicarbazone using computational calculations. *J Phys Chem Solids* 91: 55-68.
8. Xavier S, Periandy S (2015) Spectroscopic (FT-IR, FT-Raman, UV and NMR) investigation on 1-phenyl-2-nitropropene by quantum computational calculations. *Spectrochim Acta A Mol Biomol Spectrosc*. 149: 216-230.

9. Moorthy N, Prabakar PJ, Ramalingam S, Govindarajan M, Gnanamuthu SJ (2016) Spectroscopic analysis, AIM, NLO and VCD investigations of acetaldehyde thiosemicarbazone using quantum mechanical simulations. *J Phys Chem Solids*. 95: 74-88.
10. Hiremath CS, Yenagi J, Tonannavar J (2007) FT-Raman and infrared spectra and vibrational assignments for 3-chloro-4-methoxybenzaldehyde, as supported by ab initio, hybrid density functional theory and normal coordinate calculations. *Spectrochim Acta A Mol Biomol Spectrosc*. 68: 710-717.
11. George G, Ramalingam S, Periandy S, Gokulakrishnan V (2016) Spectroscopic investigation and chemical properties analysis on anticancer compound; α , α , α , α -Tetrabromo-p-Xylene with computational analysis. *J Mol Struct* 1106: 37-52.
12. Ali MM, George G, Ramalingam S, Periandy S, Gokulakrishnan V (2015) Vibrational [FT-IR, FT-Raman] analysis, NMR and mass-Spectroscopic investigation on 3, 6-Dimethylphenanthrene using computational calculation. *J Mol Struct* 1099: 463-481.
13. Rauhut G, Pulay P (1995) Transferable scaling factors for density functional derived vibrational force fields. [Erratum to document cited in CA122:199802]. *J. Phys. Chem* 99: 14572-14572.
14. Meyer W, Pulay P (1974) Hartree-Fock calculation of the harmonic force constants and equilibrium geometry of formaldehyde. *Theoretica Chimica Acta* 32: 253-264.
15. Hameka HF, Famini GR, Jensen JO, Newhouse EI (1990) Computations of vibrational infrared frequencies of selected amines. *Pennsylvania Univ Philadelphia*
16. Ebenezar JD, Ramalingam S, Raja CR, Helan V (2013) Precise spectroscopic [IR, Raman and NMR] investigation and gaussian hybrid computational analysis (UV-visible, NIR, MEP Maps and Kubo Gap) on L-valine. *J Theor Comput Sci* 1: 1-3.
17. Varsányi G (1974) Assignments for vibrational spectra of 700 benzene derivatives. Hilger.
18. Socrates G (2004) Infrared and Raman characteristic group frequencies: tables and charts. John Wiley & Sons.
19. Becke AD (1993) Density-functional thermochemistry. III. The role of exact exchange. *J Chem Phys* 98: 5648-5652.
20. Altun A, Gölcük K, Kumru M (2003) Structure and vibrational spectra of p-methylaniline: Hartree-Fock, MP2 and density functional theory studies. *J Mol Struct-Theochem* 637: 155-169.
21. Muthu S, Ramachandran G (2012) Vibrational spectroscopic investigation on the structure of 2-ethylpyridine-4-carbothioamide. *Spectrochim Acta A Mol Biomol Spectrosc* 93: 214-222.
22. Dani VR (1995) *Organic Spectroscopy*. Tata McGraw- Hill publishing company, New Delhi.
23. Singh RN, Kumar A, Tiwari RK, Rawat P (2013) Study of spectroscopic, reactivity and NLO properties of synthesized dipyrromethane containing cyanovinylhydrazide using experimental and theoretical approaches. *J Mol Struct*. 1048: 448-459.
24. Kalsi PS (1993) *Spectroscopy of Organic Compounds*, Wiley Eastern Limited, New Delhi.
25. Ramalingam S, Periandy S (2011) Spectroscopic investigation, computed IR intensity, Raman activity and vibrational frequency analysis on 3-bromoanisole using HF and DFT (LSDA/MPW1PW91) calculations. *Spectrochim Acta A Mol Biomol Spectrosc* 78: 835-843.
26. Cotlhup NB, Daly LH, Weberly SE (1964) *Introduction to Infrared and Raman Spectroscopy*, Academic Press, Inc, New York.
27. Sundaraganesan N, Kumar KS, Meganathan C, Joshua BD (2006) Vibrational spectroscopy investigation using ab initio and density functional theory analysis on the structure of 2-amino-4, 6-dimethoxypyrimidine. *Spectrochim Acta A Mol Biomol Spectrosc* 65: 1186-1196.
28. Babu VA, Lakshmaiah B, Ramulu KS, Rao GR (1987) Substituted Benzenes. 13. Normal Coordinate Analysis of Anisoles. *Indian j pure appl phy* 25: 58-65.
29. Abood NA, AL-Askar M, Saeed BA (2012) Structures and vibrational frequencies of Imidazole, benzimidazole and its 2-alkyl Derivatives determined by DFT Calculations. *Basrah Journal of Science* 30: 119-131.
30. Shakila G, Periandy S, Ramalingam S (2011) Molecular structure and vibrational analysis of 3-Ethylpyridine using ab initio HF and density functional theory (B3LYP) calculations. *Spectrochim Acta A Mol Biomol Spectrosc* 78: 732-739.
31. Gamer G, Wolff H (1973) Raman and infrared spectra of gaseous secondary aliphatic amines [(CH₃2NH, (CH₃)₂ND, (C₂H₅)₂NH and C₂H₅NHCH₃]. *Spectrochim Acta A* 29: 129-137.
32. Stewart JE (1959) Vibrational spectra of primary and secondary aliphatic amines. *J Chem Phys* 30: 1259-1265.
33. Sharma BK (2000) *Instrumental Methods of Chemical Analysis*, Krishna Prakashan Media 110-150.
34. Spire A, Barthes M, Kellouai H, De Nunzio G (2000) Far-infrared spectra of acetanilide revisited. *Physica D* 137: 392-401.
35. Silverstein M, Webster FX (2003) *Spectrometric Identification of Organic Compounds* (6th edn) John Wiley, Asia 75-105.
36. Bellamy LJ (1975) *The Infrared Spectrum of Complex Molecules* (3rd edn), Chapman and Hall, London.
37. Karunakaran V, Balachandran V (2014) Experimental and theoretical investigation of the molecular structure, conformational stability, hyperpolarizability, electrostatic potential, thermodynamic properties and NMR spectra of pharmaceutical important molecule: 4'-Methylpropiofenone. *Spectrochim Acta A Mol Biomol Spectrosc* 128: 1-4.
38. Madanagopal A, Periandy S, Gayathri P, Ramalingam S, Xavier S (2017) Molecular structure activity on pharmaceutical applications of Phenacetin using spectroscopic investigation. *J Mol Struct* 1127: 611-625.
39. Al-Sehemi AG, Irfan A, Alrumman SA, Hesham AE (2016) Antibacterial activities, DFT and QSAR studies of quinazolinone compounds. *Bull Chem Soc Ethiop* 30: 307-316.